




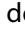









Assessment of PD-L1 expression across breast cancer molecular subtypes, in relation to mutation rate, *BRCA1*-like status, tumor-infiltrating immune cells and survival

Marcelo Sobral-Leite ^{a,b}, Koen Van de Vijver ^c, Magali Michaut ^d, Rianne van der Linden^c, Gerrit K.J. Hooijer^e, Hugo M. Hurlings ^c, Tesa M. Severson ^d, Anna Marie Mulligan^{f,g}, Nayana Weerasooriya ^h, Joyce Sanders ^c, Annuska M Glas ⁱ, Diederik Wehkampⁱ, Lorenza Mittempergherⁱ, Kelly Kersten[#], Ashley Cimino-Mathews^k, Dennis Peters^l, Erik Hooijberg ^c, Annegien Broeks^l, Marc J. van de Vijver^e, Rene Bernards ^d, Irene L. Andrulis^{g,m,n}, Marleen Kok ^{o,p}, Karin E. de Visser ⁱ, and Marjanka K. Schmidt ^a

^aDivision of Molecular Pathology, Netherlands Cancer Institute, Amsterdam, The Netherlands; ^bCoordenação de Pesquisa, Instituto Nacional de Câncer, Rio de Janeiro, RJ, Brasil; ^cDepartment of Pathology, Netherlands Cancer Institute, Amsterdam, The Netherlands; ^dDivision of Molecular Carcinogenesis, Oncode Institute, Netherlands Cancer Institute, Amsterdam, The Netherlands; ^eDepartment of Pathology, Academic Medical Center, Amsterdam, The Netherlands; ^fLaboratory Medicine Program, University Health Network, Toronto, ON, Canada; ^gDepartment of Laboratory Medicine and Pathobiology, University of Toronto, Toronto, ON, Canada; ^hUniversity Health Network, Toronto, ON, Canada; ⁱAgendia NV, Science Park, Amsterdam, The Netherlands; ^jDivision of Tumor Biology and Immunology, Oncode Institute, Netherlands Cancer Institute, Amsterdam, The Netherlands; ^kDepartments of Pathology and Oncology, The Johns Hopkins Hospital, Baltimore, USA; ^lCore Facility Molecular Pathology and Biobanking, Division of Molecular Pathology, Netherlands Cancer Institute, Amsterdam, The Netherlands; ^mLunenfeld-Tanenbaum Research Institute, Sinai Health System, Toronto, Canada; ⁿDepartment of Molecular Genetics, University of Toronto, Toronto, ON, Canada; ^oDivision of Molecular Oncology and Immunology, Netherlands Cancer Institute, Amsterdam, The Netherlands; ^pDivision of Medical Oncology, Netherlands Cancer Institute, Amsterdam, The Netherlands

ABSTRACT

To better understand the expression pattern of programmed death-ligand 1 (PD-L1) expression in different breast cancer types, we characterized PD-L1 expression in tumor and tumor-infiltrating immune cells, in relation to mutation rate, *BRCA1*-like status and survival. We analyzed 410 primary treatment-naïve breast tumors comprising 162 estrogen receptor-positive (ER+) and HER2-, 101 HER2+ and 147 triple-negative (TN) cancers. Pathologists quantified tumor-infiltrating lymphocytes (TILs) and PD-L1 expression in tumor cells and TILs using whole slides and tissue microarray. Mutation rate was assessed by DNA sequencing, *BRCA1*-like status using multiplex ligation-dependent probe amplification, and immune landscape by multiplex image analyses of CD4, CD68, CD8, FOXP3, cytokeratin, and PD-L1. Half of PD-L1 scores evaluated by tissue microarray were false negatives compared to whole slide evaluations. We observed at least 1% of PD-L1-positive (PD-L1+) cells in 53.1% of ER+HER2-, 73.3% of HER2+, and 84.4% of TN tumors. PD-L1 expression was higher in ductal compared to lobular carcinomas, also within ER+HER2- tumors ($p = 0.04$). High PD-L1+ TILs score ($> 50\%$) was independently associated with better outcome in TN tumors (HR = 0.27; 95%CI = 0.10–0.69). Within TN tumors, PD-L1 and TIL scores showed a modest but significant positive association with the number of silent mutations, but no association with *BRCA1*-like status. Multiplex image analyses indicated that PD-L1 is expressed on multiple immune cells (CD68+ macrophages, CD4+, FOXP3+, and CD8+ T cells) in the breast tumor micro-environment, independent of the PD-L1 status of the tumor cells. We found no evidence that levels of PD-L1 + TILs in TN breast cancer are driven by high mutation rate or *BRCA1*-like status.

ARTICLE HISTORY

Received 30 April 2018
Revised 3 August 2018
Accepted 4 August 2018



KEYWORDS

Breast cancer; PD-L1; TILs; mutations; *BRCA1*-like

Introduction

The presence of tumor-infiltrating lymphocytes (TILs) has been associated with favorable clinical outcomes in triple-negative (TN) and human epidermal growth factor receptor 2 positive (HER2+) breast cancer¹, but not in estrogen receptor (ER) positive breast cancer.² TIL density and composition show considerable heterogeneity between and within tumors, but the factors that determine this variation are unknown.³

Programmed cell death 1 (PD-1), a transmembrane protein, plays an important role in down-regulating the immune system.⁴ One of the PD-1 ligands, programmed death-ligand 1 (PD-L1), can be expressed on tumor and immune cells.⁵ PD-L1/PD-1 binding physiologically promotes immune-tolerance in peripheral tissues.^{4,5} This signaling pathway is used by tumor cells to inhibit antitumor immunity.⁴⁻⁷ Various cancer types express PD-L1 at different levels.^{8,9}


CONTACT Marjanka K. Schmidt  mk.schmidt@nki.nl  Division of Molecular Pathology, Netherlands Cancer Institute, Plesmanlaan 121 - 1066CX Amsterdam, The Netherlands

Present address of Koen Van de Vijver is Ghent University Hospital, Ghent, Belgium.

Present address of Magali Michaut is Biotech Research & Innovation Centre, Københavns Universitet, Copenhagen, Denmark.

Present address of Kelly Kersten is Department of Pathology, University of California, San Francisco, USA.

[#]Department of Pathology, University of California, San Francisco, USA

 Supplementary data can be accessed [here](#)

Immunomodulatory agents blocking the PD-1/PD-L1 axis have shown effectiveness in melanoma, lung, and other cancer types, including breast.¹⁰⁻¹⁴ However, the response to anti-PD-1/PD-L1 therapy varies significantly among patients.¹⁰⁻¹⁴ According to clinical studies, response rates to anti-PD-1/PD-L1 therapy range between 5 to 23% within advanced TN breast cancer patients.¹⁵ Higher response rates are linked with PD-L1 positivity.¹⁵ However, not all PD-L1-positive (PD-L1+) tumors respond to anti-PD-1/PD-L1 therapy.

In breast cancer, previous studies reported high TIL density, PD-L1 expression and mutation rate in TN tumors, compared with other subtypes.¹⁶⁻³⁰ However, it is still unknown whether the mutation rate of breast tumor cells contributes to the tumor infiltration of immune cells and PD-L1 expression.^{3,31} Moreover, the association between PD-L1 expression and prognosis of breast cancer remains controversial.^{8,9,18-29} Thus, further studies on PD-L1 expression and other potential biomarkers, such as but not limited to TIL density and CD8 expression, are clearly needed.¹⁴ Moreover, most observational studies have measured PD-L1 expression in breast cancer using tissue microarrays (TMAs) potentially limiting their conclusions.¹⁸⁻²⁷

The overall aim of this study was to perform a comprehensive evaluation of PD-L1 expression in breast tumor cells and tumor-associated immune cells. We also compared PD-L1 scoring on whole slide sections versus TMAs. To address this aim, we measured PD-L1 expression in various tumor-infiltrated immune cell types using an immunofluorescent multiplex approach; we investigated if TIL density or PD-L1 expression in TN tumors varies according to somatic mutation rate or surrogate homologous recombination deficiency status (*BRCA1*-like status); and we examined whether levels of TIL density and PD-L1 expression are associated with survival within different breast cancer subtypes (ER+HER2-, HER2+, and TN).

Results

Underestimation of PD-L1 positivity using TMAs

Initially, we examined whether PD-L1 expression analysis using TMAs would satisfactorily represent the extent of PD-L1 expression of whole tumor sections. Each TMA consisted of tumor cores measuring 1.4 mm in diameter; with 3 to 6 cores per tumor. PD-L1 scores of 118 tumors from the ONCOPOOL cohort were used to compare TMA with whole slide observations, which showed that 49% of the TMA tumor results were false negatives. Generally, scores obtained by TMA did not reflect those obtained by whole slides (figures 1A-C, $ICC_{PD-L1+TILs} = 0.27$; 95%CI = 0.13–0.40). It appeared that often the TMA cores were not taken close enough to the invasive tumor front, where PD-L1 positivity was more frequently detected (figures 1D-H and supplementary figure 1). Therefore, in this study, TIL density and PD-L1 expression for further analyses were based on measurements using whole slides.

Variation in PD-L1 expression among tumors is related to the extent of the presence of TILs

In total, 410 breast tumors were scored for TIL density and PD-L1 expression (clone E1L3N XP®, Cell Signaling; see supplementary materials and methods). Consistent with other studies,^{1,2,16,19,32} TIL density was higher in TN tumors than in other tumor subtypes ($p < 0.0001$; figure 2A). We observed at least 1% of PD-L1-positive (immune or tumor) cells in 53.1% of ER+HER2-, 73.3% of HER2+, and 84.4% of TN tumors (Table 1). Tumors with < 5% TILs were negative for PD-L1+ TILs (figure 2B and 3A). Overall, TIL density and PD-L1+ TILs score showed strong correlation (Spearman's coefficient: $r = 0.83$; supplementary figure 2). We found that PD-L1 positivity in tumor cells was mainly detected when the tumor cells were surrounded by PD-L1+ TILs (figure 3B). On the other hand, most of the tumors (or tumor areas) containing PD-L1+ TILs did not contain any PD-L1+ tumor cells. PD-L1+ tumor cells were present in 11.1% of ER+HER2-, 31.7% of HER2+, and 38.1% of TN tumors. However, most of these tumors exhibited PD-L1+ tumor cells in less than 25% of the observed area (figure 2C).

The intensity of the PD-L1 staining and its spatial location were also associated with the percentage of PD-L1 positivity (figure 2D and 2E). We observed three main immune infiltration patterns based on TIL density, PD-L1 expression, and histological organization: (i) tumors containing focal PD-L1+ TILs showed predominant weak to mild intensity of PD-L1 staining in the stroma with no PD-L1+ tumor cells (3C and 3D); (ii) PD-L1+ TILs located predominantly near the invasive tumor front, with no or very focal PD-L1+ tumor cells (3E and 3F); and (iii) tumors classified as containing high PD-L1+ TILs showed mild to strong intensity of a diffuse intratumoral PD-L1 staining (including few PD-L1+ tumor cells), located at the invasive tumor front and within the tumor margins (3G and 3D).

Tumor features are associated with PD-L1 expression

We investigated which tumor characteristics were associated with PD-L1 expression, in addition to the lack of ER, PR and HER2 expression (Table 1 and supplementary figure 3A). Invasive lobular carcinomas had lower PD-L1 expression compared with invasive breast carcinomas of no special type, previously known and further referred to as invasive ductal carcinomas ($p < 0.0001$; figure 2F) with an odds ratio (OR) from multivariable logistic regression analysis of 0.43; 95%CI = 0.18–0.97, supplementary figure 3A). Results were similar in ER+HER2- tumors ($p = 0.042$; Table 1 and $OR_{ER+HER2-/lobular} = 0.35$; 95%CI = 0.13–0.90, supplementary figure 3B). Consistent with previous publications,^{8,17-21,25,29} poor tumor grade was strongly associated with PD-L1 expression in HER2+ and TN tumors (figure 2G, Table 1 and supplementary figure 3A, C and D). In contrast, we did not observe an association between grade and PD-L1 expression in the ER+HER2- group (Table 1 and supplementary figure 3B).

The same PD-L1 and TIL analyses using whole slides of tumor sections from an independent cohort ($n = 144$) from Canada (OFBCR) showed similar expression profiles and associations as observed in the Dutch cohorts (supplementary Table 1 and supplementary figure 4).

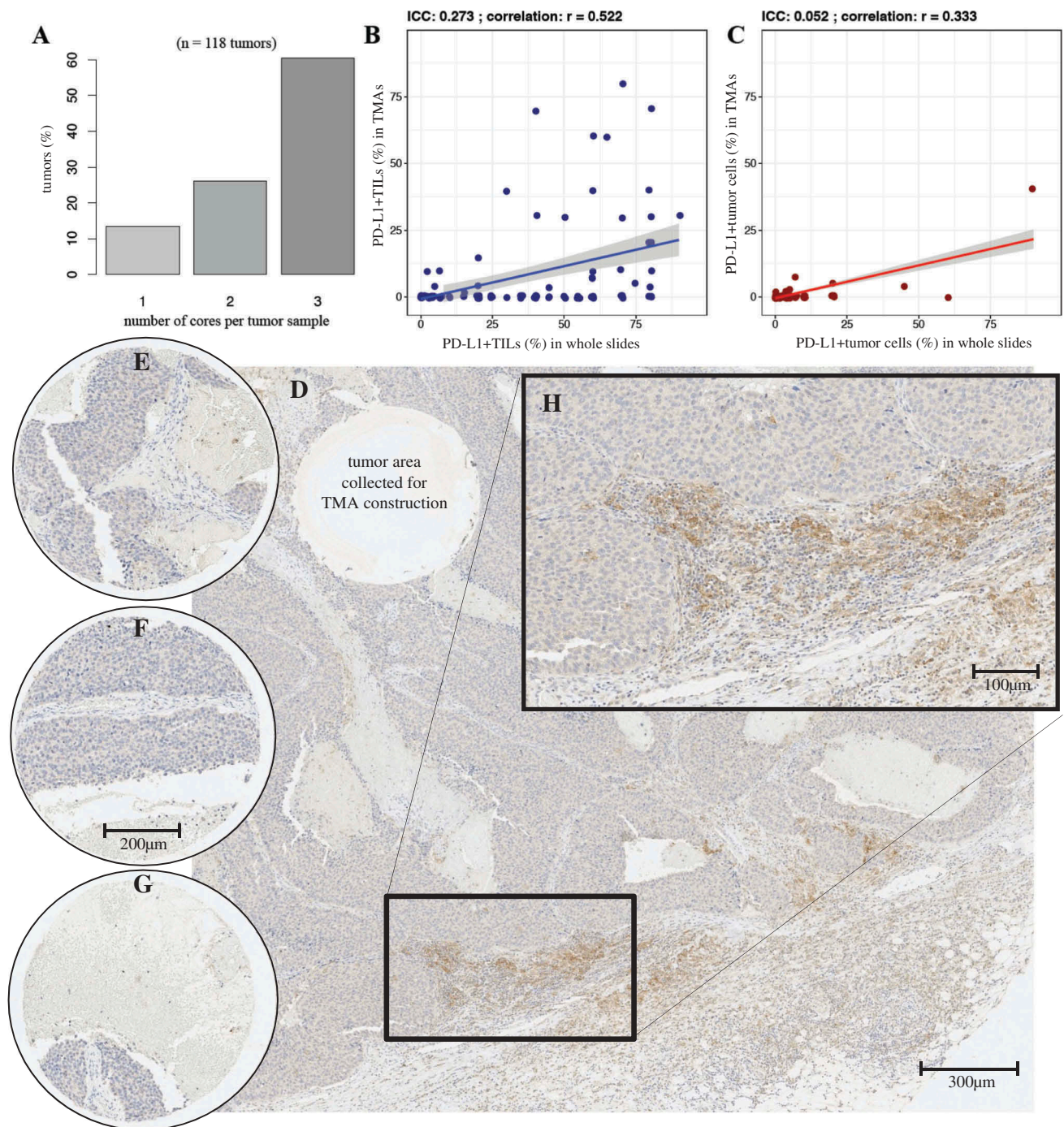


Figure 1. High number of PD-L1 negative scores were detected using TMAs. In total, 118 tumors from the ONCOPOOL cohort were scored using TMA and whole slides. A) Around 85% of the tumor contributed with 2 or 3 cores of 0.6 mm for the scores using TMA. B) The scores of PD-L1+ TILs generated using TMA showed poor correlation with those generated by whole slides observation. C) Comparison of the scores of PD-L1+tumor cells generated by TMA and whole slides also showed poor correlation. D) Example of false negative score obtained by TMA analysis. TMA cores were negative for PD-L1 staining using immunohistochemistry assays (E, F and G); however, the PD-L1 positive cells were located away from the area where the cores were taken for TMA construction. Area of PD-L1+TILs detailed in H. Calculation: intraclass correlation coefficient (ICC) and Spearman correlation (r). Lines in B and C represent the linear correlation; the gray area around the line represents the standard error. Abbreviations: tissue microarray (TMA), PD-L1+tumorinfiltrating lymphocytes (PD-L1+TILs).

Breast tumor associated-lymphocytes and macrophages exhibit PD-L1 expression

TILs are composed of several types of lymphocytes and are surrounded by other immune cells present in the tumor microenvironment.^{16,33} Using multiplex IF staining, we investigated if a specific immune cell type would demonstrate a predominant proportion of PD-L1+ cells more

than other immune cell types. We applied image analysis on the immune-infiltrate areas of seven ER-negative tumors representing examples of three types of immune infiltration patterns (based on TIL organization and PD-L1 expression levels as described above; figure 3). One pathologist (HH) chose five areas from each tumor, including tumor cells and the adjacent microenvironment (supplementary table 2).

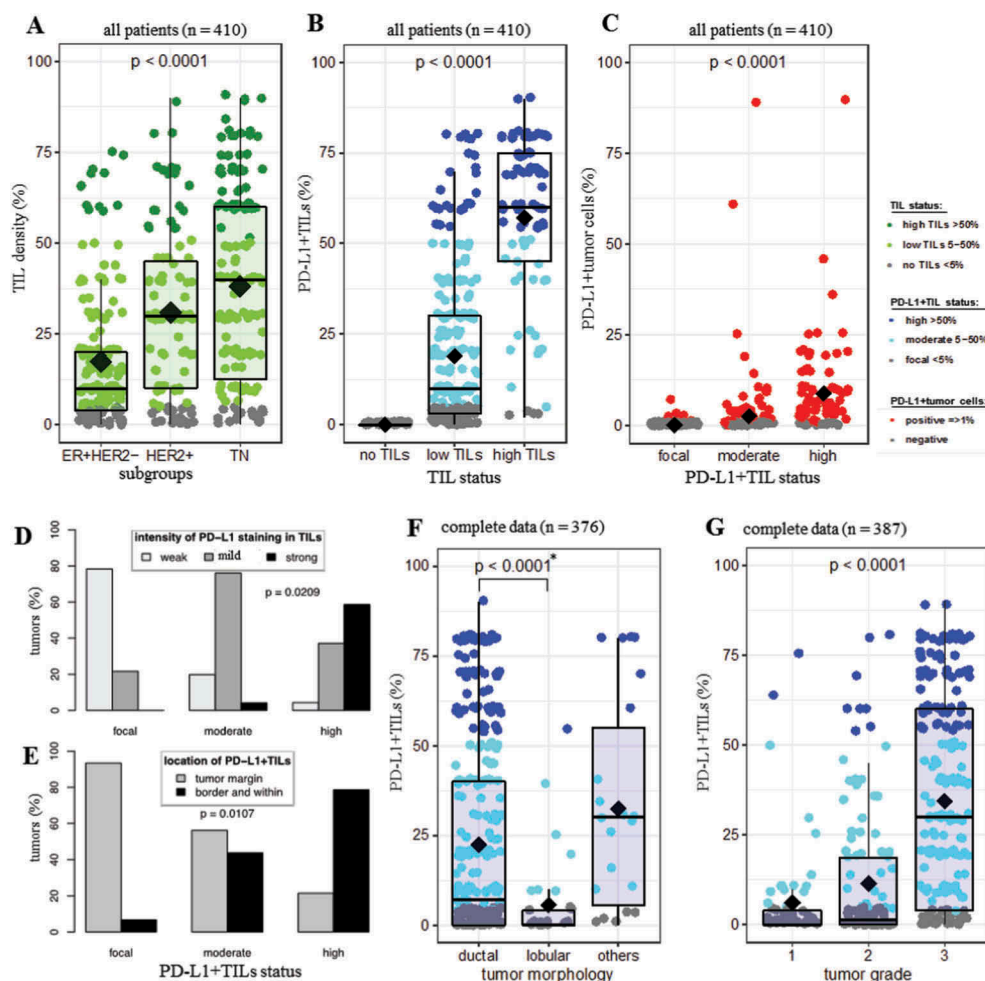


Figure 2. PD-L1 expression is associated with specific breast tumor characteristics. A) Tumor-infiltrating lymphocyte (TIL) density was higher in TN tumors. B) PD-L1+TIL score increased according to the higher status of TILs. C) PD-L1+tumor cells were more frequent in tumors with high PD-L1+TILs. Tumors classified as high PD-L1+TILs had a stronger intensity of staining (D) and were predominantly located at the border and within the tumor margins (E), compared with tumors classified as focal and moderate PD-L1+TILs. F) Lobular carcinomas had lower levels of PD-L1+TILs compared with ductal carcinomas. G) Tumor-infiltration of PD-L1+lymphocytes were more extensive in high grade tumors. The average mean of each distribution is represented by a lozenge. Comparisons of means were tested by ANOVA. (*) Comparison between the means of ductal and lobular groups by Student's t-test. Categorical levels of each score are defined in the legend and represented by degrees of green (%TIL density), blue (%PD-L1+TILs) or red (%PDL1+ tumor cells). Abbreviations: estrogen receptor (ER), tumor-infiltrating lymphocytes (TILs).

We analyzed two tumors (pattern i) containing dense aggregates of TILs exhibiting focal PD-L1 expression and surrounded by well-delimited area of tumor cells (figure 4A). We detected CD4+, CD8+ and FOXP3+ T lymphocytes, and few macrophages CD68+ (figure 4B). Image analysis showed weak PD-L1 expression (figure 4C) in a small percentage of these immune cells (0.1–4.7%; supplementary table 2). PD-L1+ immune cells were located in the stroma and away from any PD-L1+ tumor cells (figure 4A and B).

Another typical pattern of lymphocytic infiltration (ii) is very often observed at the invasive tumor front (figure 4D). We identified a diverse immune-cell type composition at the interface between tumor cells and regions of dense stromal TILs (figure 4E), where moderate to strong PD-L1 staining in tumor and immune cells was observed (figure 4F). Image analysis of three tumors containing this particular pattern revealed PD-L1 positivity in a proportion of the lymphocytes (5.5–14.6%), macrophages (6.2%) and tumor cells (13.6%; supplementary table 2).

The analyses of two tumors containing abundant lymphocytic infiltration in the stroma and in the intratumoral compartments (pattern iii) showed intense and diffuse PD-L1 staining (figure 4G). These tumors showed a mixed immune cell composition not only in the stroma, but also in the intratumoral compartment (figure 4H). We detected a high proportion of intense PD-L1 expression among all cell types (18.8–45.7% of lymphocytes, 26.8% of macrophages and 75.5% of tumor cells; supplementary table 2 and figure 4I).

Taking together, these analyses suggest that a proportion of various types of lymphocytes, e.g. CD4+, CD8+ and FOXP3+ T cells; as well as CD68+ macrophages express PD-L1 (figure 4). The data also indicated that the tumors with a diffuse/intratumoral immune pattern also have the highest proportion of PD-L1 positive (immune and tumor) cells (supplementary table 2).

Table 1. Comparison of patient and tumor characteristics, and PD-L1 status in each breast cancer subgroup.

Clinical and pathological characteristics	PD-L1		PD-L1		P value	PD-L1		PD-L1		P value	PD-L1		PD-L1		P value
	negative		positive			negative		positive			negative		positive		
	n	%	n	%		n	%	n	%		n	%	n	%	
TILs					< 0.001					< 0.001					< 0.001
< 5%	44	100.0	0	0.0		20	100.0	0	0.0		19	100.0	0	0.0	
5–50%	32	30.2	74	69.8		7	11.9	52	88.1		4	5.1	74	94.9	
> 50%	0	0.0	12	100.0		0	0.0	22	100.0		0	0.0	50	100.0	
Morphology type					0.042					0.066					0.176
ductal	56	42.7	75	57.3		24	25.8	69	74.2		12	13.6	76	86.4	
lobular	18	69.2	8	30.8		3	75.0	1	25.0		1	33.3	2	66.7	
others	2	40.0	3	60.0		0	0.0	4	100.0		0	0.0	12	100.0	
unknown											10	22.7	34	77.3	
Tumor grade					0.763					< 0.001					0.002
grade 1	23	46.0	27	54.0		8	72.7	3	27.3		1	50.0	1	50.0	
grade 2	34	50.7	33	49.3		12	46.2	14	53.8		8	38.1	13	61.9	
grade 3	18	43.9	23	56.1		6	10.9	49	89.1		12	10.5	102	89.5	
unknown	1	25.0	3	75.0		1	11.1	8	88.9		2	20.0	8	80.0	
Tumor size					0.280					0.067					0.277
≤ 2cm	45	43.3	59	56.7		19	35.2	35	64.8		14	19.2	59	80.8	
> 2cm	31	53.4	27	46.6		8	17.0	39	83.0		8	11.3	63	88.7	
unknown															
Lymph node status					0.722					0.012					0.718
pN0	44	45.8	52	54.2		21	37.5	35	62.5		16	16.7	80	83.3	
pN1	32	50.0	32	50.0		6	13.3	39	86.7		6	12.8	41	87.2	
unknown	0	0.0	2	100.0											
ER status										0.172					
ER-						12	20.7	46	79.3						
ER+						15	34.9	28	65.1						
PR status					0.636					0.190					
PR-	7	38.9	11	61.1		17	22.7	58	77.3						
PR+	69	47.9	75	52.1		10	38.5	16	61.5						
Chemotherapy					0.592					0.321					0.423
no	66	48.2	71	51.8		21	30.4	48	69.6		16	18.2	72	81.8	
yes	10	40.0	15	60.0		6	18.8	26	81.3		7	11.9	52	88.1	
Endocrine therapy*					0.574					0.549					
yes	25	43.1	33	56.9		16	30.2	37	69.8						
no	51	49.0	53	51.0		11	22.9	37	77.1						
Radiotherapy					0.237					0.994					1.000
yes	18	58.1	13	41.9		8	28.6	20	71.4		6	15.0	34	85.0	
no	58	44.3	73	55.7		19	26.0	54	74.0		17	15.9	90	84.1	
Study															0.195
ONCOPOOL											13	12.6	90	87.4	
RATHER											10	22.7	34	77.3	

PD-L1 negative tumors classified as: absence of immune and tumor cells expressing PD-L1; and PD-L1 positive group classified as: presence of at least 1% of the immune or tumor cells showing PD-L1 expression. P value of the comparison between PD-L1 negative and PD-L1 positive groups using the Chi-square test or Fisher's exact test when table cells were smaller than 7. Unknown status of the variables was not included in the P value calculations; Note: (*) Endocrine therapy was still prescribed regardless the ER status in the period this cohort has been treated (1990–1999). Abbreviations: estrogen receptor (ER), progesterone receptor (PR), tumor-infiltrating lymphocytes (TILs).

PD-L1 expression is associated with improved prognosis in TN breast cancer

We analyzed whether TIL status and/or PD-L1 levels (in TILs or tumor cells) are related with breast cancer specific survival (BCSS), across the three breast tumor subtypes. No associations were found in the group of ER+HER2- and HER2+ tumors (figure 5A-F). As expected,^{2,34} TIL status was significantly associated with BCSS in TN tumors (multivariable model: $HR_{\text{high-TILs}} = 0.21$; 95% CI = 0.06–0.66; figure 5G and supplementary figure 5A). In TN tumors, the presence of high PD-L1+ TILs (> 50%) was also independently associated with better survival: $HR_{\text{high-PD-L1+TILs}} = 0.27$; 95%CI = 0.10–0.69; figure 5H and supplementary figure 5B). Accordingly, the presence of PD-L1+ tumor-cells was associated with improved survival, but it was not statistically significant (figure 5I and supplementary figure 5C). Analyses using distant-metastasis free survival (DMFS) as an endpoint reflected the same directions of associations as seen in the BCSS analyses (supplementary figure 6). Kaplan-Meier curves

comparing DMFS between PD-L1-low (≤ 50%) and PD-L1-high (> 50%) patients, within the groups classified either as low-TILs (≤ 50%) or high-TILs (> 50%) tumors, suggested no difference in survival (data not shown).

To further explore the association of PD-L1 expression and prognosis, we analyzed the RNA expression levels of genes encoding PD-L1 and PD-1 according to the MammaPrint risk classification. This prognostic tool is commonly used in the clinic to support clinical decisions especially in ER-positive breast cancer.³⁵ In total, we analyzed 547 breast tumors from patients included in trials in which data on the MammaPrint gene signature was collected (supplementary material and methods). The expression levels of *CD274* (PD-L1) and *PDCD1* (PD-1) were compared among high and low risk of recurrence, assessed by the MammaPrint gene expression assay,³⁶ and stratified by breast cancer molecular subtype, using Blueprint gene profile.³⁷ Among the luminal tumors (n = 490), no difference on *CD274* expression was found between high or low risk patients (supplementary figure

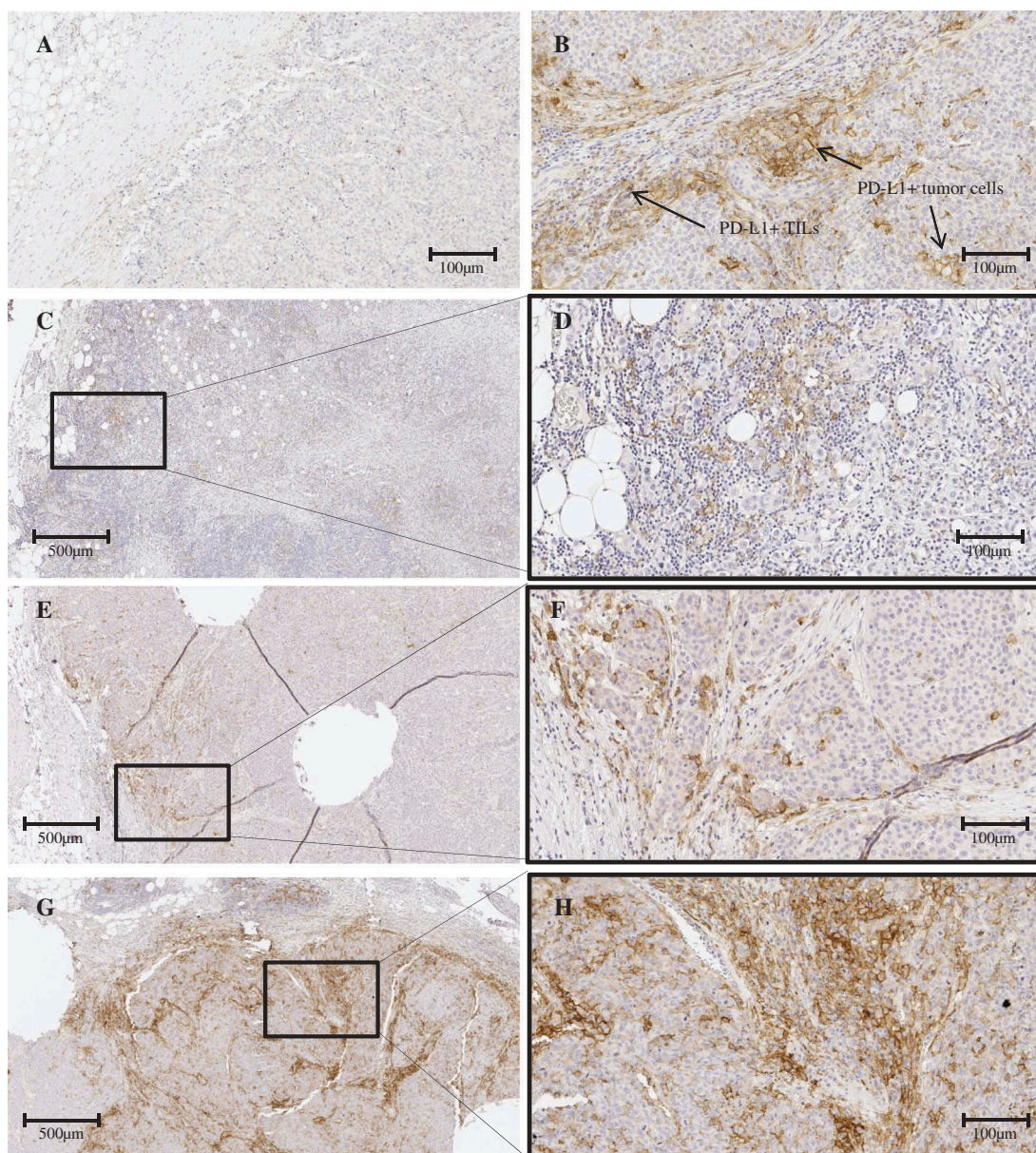


Figure 3. Representative examples of the expression of PD-L1 in primary breast tumors: A) immune desert tumor; B) PD-L1+ tumor-infiltrating lymphocytes (PD-L1+TILs) surrounded by few tumor cells with membranous PD-L1 staining. C) Tumor showing lymphocytes aggregated in the stroma, exhibiting focal PD-L1+TILs (i); detailed in D. E) Tumor showing moderate PD-L1 expression in TILs nearby the tumor invasive edge, but without PD-L1+ tumor cells (ii); detailed in F. G) Example of extensive immune infiltration (stromal and intratumoral), diffuse and intense PD-L1 expression in TILs and few tumor cells (iii); detailed in H.

7A). However, *PDCD1* expression was slightly higher in patients with MammaPrint high risk scores, compared with MammaPrint low risk patients (p -value < 0.0001; supplementary figure 7B). This adds evidence that PD-L1 expression has no prognostic value in ER-positive breast cancer.

PD-L1 status in TN breast cancer is not significantly associated with total mutation rate

In order to better describe the factors that could underlie the presence of high TILs and PD-L1 expression in TN breast cancer, we assessed the somatic mutational status of 613 cancer-related genes and *BRCA1*-like status in 56 TN tumors from the RATHER cohort. The average number of somatic mutations, of all 613 genes together, showed a trend to be increased in tumors with high TIL density or PD-L1 expression (supplementary figure 8A, 8C).

Although we observed a weak significant correlation between the number of silent somatic mutations and the increment of the scores of TILs ($r = 0.280$; $p = 0.033$; figure 6C), PD-L1+ TILs ($r = 0.296$; $p = 0.024$; figure 6D), and PD-L1+ tumor cells ($r = 0.363$; $p = 0.005$; supplementary figure 8E), the number of non-silent somatic mutations (that could potentially result in neoantigens) did not show a correlation with TILs and PD-L1 scores (figure 6A, 6B and supplementary figure 8D).

These 56 TN breast tumors were previously classified in terms of *BRCA1*-like status,^{38,39} a surrogate for homologous recombination deficiency status.^{38,39} TIL density and PD-L1 expression levels did not show significant differences according to *BRCA1*-like status, or according to *BRCA1* or *BRCA2* somatic mutation status (figure 6E-G and supplementary figure 9A-F). We also did not find any specific gene in which the mutation status was associated with TIL density or PD-L1 expression levels (data not shown).

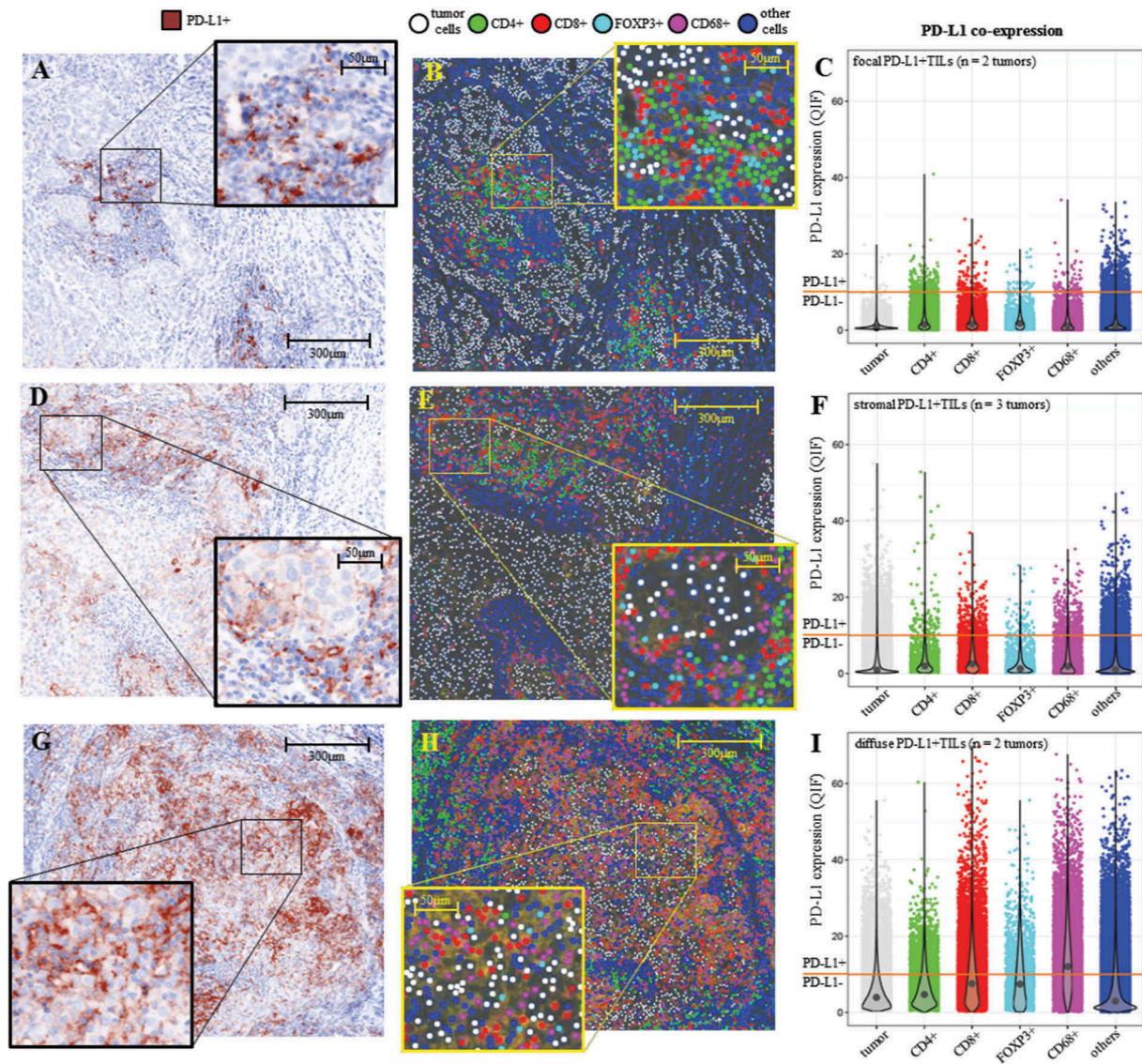


Figure 4. Distribution of PD-L1 expression among the immune cell types. Bright field images of PD-L1 immunofluorescent staining of three different immune infiltration patterns and PD-L1+TIL status were selected: i) lymphocytic aggregates/focal PD-L1+TILs in A), ii) stromal PD-L1+TILs at the invasive margins in D) and iii) diffuse/intratumoral PD-L1+TIL infiltration in G). Areas containing tumor cells and adjacent microenvironment were detailed. Color-based maps of these areas revealed the single-cell phenotype in the image generated by imaging analysis software (C, F and H): tumor cells (white); CD4 (green), CD8 (red), FOXP3 (cyan), CD68 (magenta), and other cells (blue). Distribution of the quantitative immunofluorescence (QIF) of PD-L1 expression, per cell phenotype, revealed the proportion of PD-L1+cells in each tumor. Orange lines correspond to the threshold for PD-L1 classification as negative (QIF < 7) or positive (QIF ≥ 7). Violin plots show the distribution and mean of PD-L1 QIF scores per cell phenotype. Cells classified as 'others' represent other cell types in the stroma compartment that could not be phenotype due the lack of specific markers.

Discussion

The present study examines PD-L1 expression profiles and their associations with pathological variables, genetic features, and clinical outcome across the main breast cancer subtypes of breast cancers by analyzing whole tissue sections. In order to better understand the immune biology components of PD-L1 and TIL organization in breast tumors, we performed *per cell* image phenotyping and measured the proportion of PD-L1+ cells in each phenotype. We demonstrated that a proportion of CD4+ helper T cells, CD8+ cytotoxic T cells, FOXP3+ T regulatory cells and CD68+ macrophages, co-express PD-L1, regardless of the pattern of immune infiltration (e.g. focal or diffuse/intratumoral PD-L1 + TILs: [figure 4](#) and supplementary table 2). These co-expression

findings in human tumors are supported by other studies using *in vitro* or other methods.^{4,5,16,40} Accordingly, our data suggest that PD-L1 expression is increased in all of these immune cell types when the immune infiltration is extensive. These data are consistent with previous studies suggesting that the PD-L1/PD-1 pathway plays a major role in the induction and maintenance of immunological exhaustion in the breast tumor microenvironment.^{4-6,14,17,33} Further development of image analysis using larger sample sets is crucial to better dissect the composition of the infiltrates, which may lead to the identification of signatures reflecting the immune recognition status of breast tumor cells.

We studied the association of PD-L1 expression with the number of mutations and *BRCA1*-like status in the TN

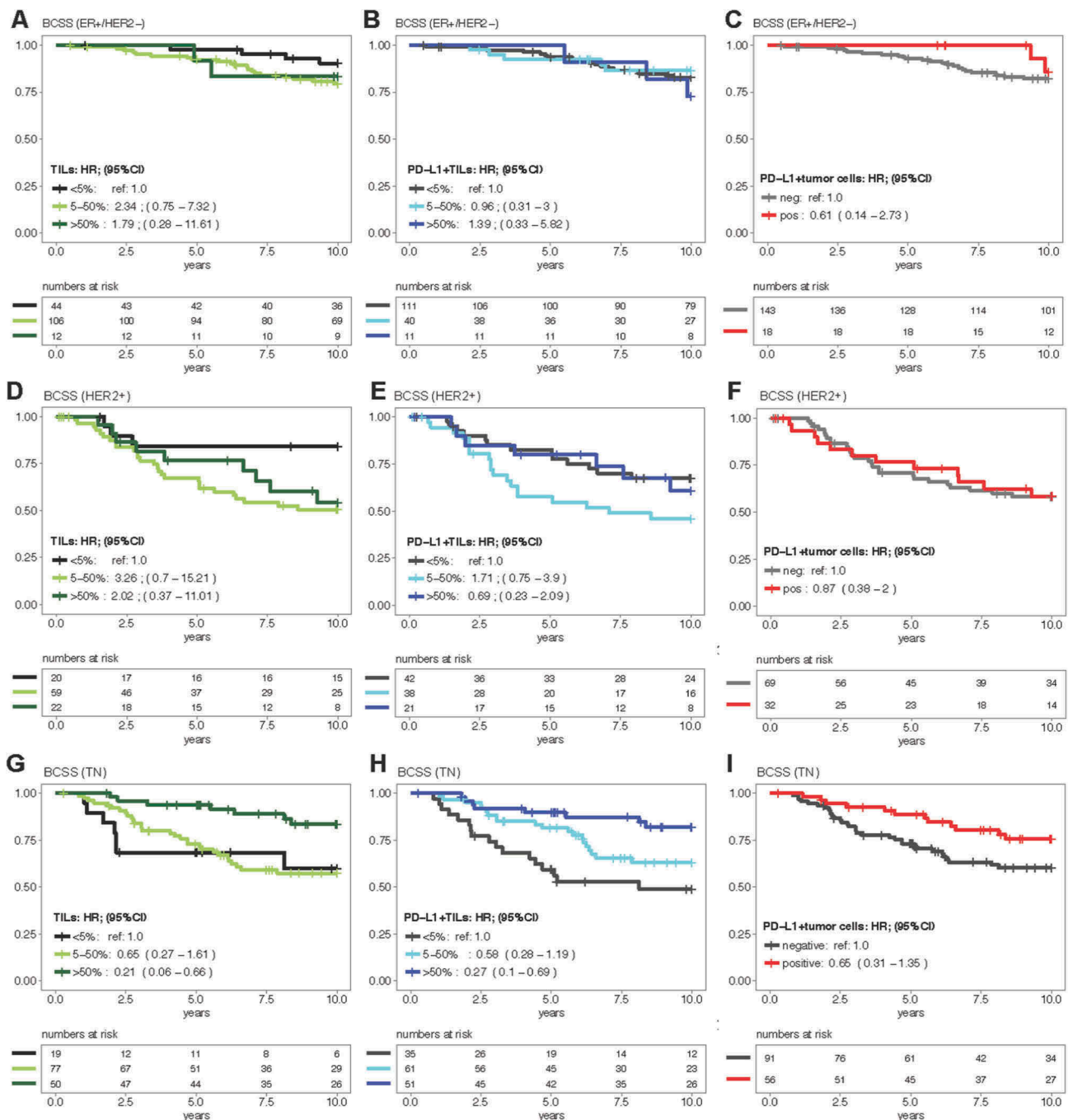


Figure 5. Association between PD-L1 expression and breast cancer specific survival (BCSS). Kaplan–Meier curves, the numbers at risk and adjusted hazard ratios (HR) of the categories of tumorinfiltrating lymphocytes (TILs), PD-L1+TILs, and PD-L1+tumor cells in ER+HER2– (A, B and C), HER2+ (D, E and F), and triple-negative (TN) tumors (G, H, I). HR based on Cox multivariable regression models were adjusted for: age at diagnosis, pathological features and adjuvant treatments (as described in the methods). Abbreviations: breast cancer specific survival (BCSS), hazard ratios (HR), 95% confidence interval (95%CI), estrogen receptor (ER), triple-negative (TN) and tumor-infiltrating lymphocytes (TILs).

tumors. There is an urgent need to understand how non-synonymous mutations in tumors could influence the anti-tumor immune response.^{3,31,33,41} Here we explored the TIL density and PD-L1 expression according to the number of somatic mutations of a 613 gene panel. No strong association was found between TIL density, PD-L1 expression and high mutation rate (supplementary figure 8A-C). Luen et al

reported similar results in a study in all breast tumor subtypes.³¹ They also did not find a significant association between the number of somatic genomic/exomic single nucleotide variants and TIL density.³¹ Increased levels of tumor immune-infiltration might be related to specific gene mutation signatures⁴¹ or mutant-specific neoantigens,⁴² which we were unable to uncover using our specific gene set. Despite

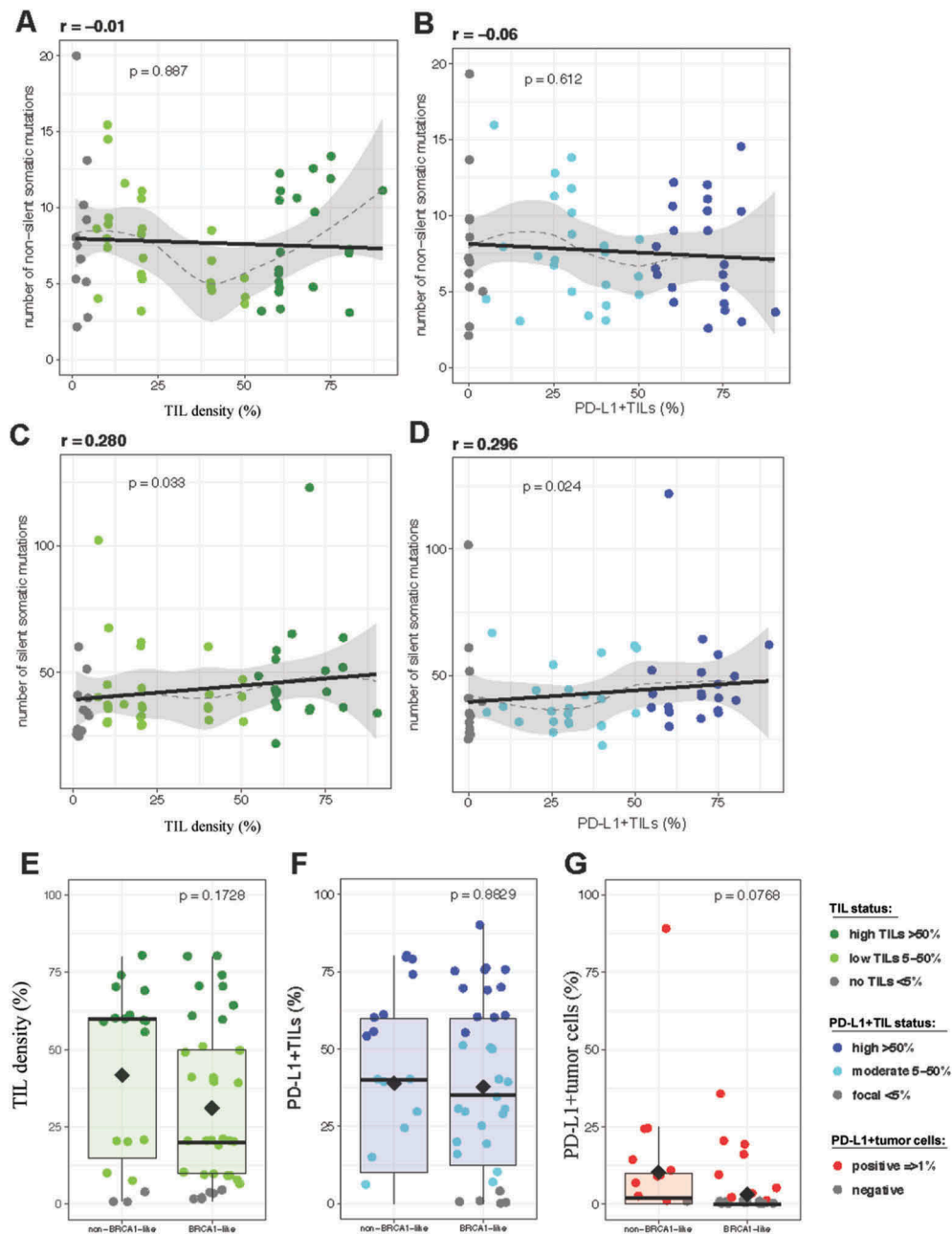


Figure 6. Mutational load and BRCA1-like status in triple-negative (TN) breast cancer (n=56). No correlation was found between the number of nonsilent somatic mutations and percentage of tumor-infiltrating lymphocyte (TIL) density (A) or percentage of PD-L1+TILs (B). Silent somatic mutations were weakly positive associated with TIL density (C) and percentage of PD-L1+TILs (D). No difference in TIL density (E), percentage of PD-L1+TILs (F) or PD-L1+ tumor cells (G) was found between non-BRCA1-like and BRCA1-like tumors. Spearman's coefficient (r) and its statistical significance (p) were used as statistical test. Dashed lines in the graphs represent the estimation of the smoothed conditional mean between the points in the graph. The gray area around the line is the estimated standard error of the smoothed mean. Linear correlation is plotted in black. Comparisons of means between two groups were examined by Student's *t* test. Abbreviations: percentage (%) and tumor-infiltrating lymphocytes (TILs).

the limited sample size and selected gene sequencing coverage, based on our results we did not find that levels of TILs and PD-L1 expression in TN breast cancer are related to high somatic mutation rate *per se*. Extensive research on potential drivers of tumor-specific immune response and the characterization of such immune profiles is needed.

PD-L1 was most significantly associated with the TN high-grade tumor subtype. But our data did not reveal a significant association between PD-L1 or TIL scores and BRCA1-like status, BRCA1, or BRCA2 mutation status in TN tumors (figure 6E, F and supplementary figure 9). In contrast to our results, Nolan et al found that BRCA1-mutated TN breast cancers (n = 29)

contained a higher number of TILs compared to wild-type breast cancers (n = 64), using data from The Cancer Genome Atlas (TCGA).⁴⁰ However, in line with our findings, Turajlic et al did not observe a correlation between TIL density and BRCA1 mutation status within TN breast tumors.⁴² Solinas et al analyzed TN tumors of 44 patients with BRCA1 or BRCA2 germline mutations and 41 patients with BRCA-wild-type breast cancers and did not observe differences in TIL density and PD-L1 expression according to BRCA1 or BRCA2-mutation status.⁴³ These results suggest that other mechanisms different from, or in addition to, high mutation rate and BRCA1-deficiency may regulate immune infiltration in TN breast cancer.

We observed a lower level of TILs and PD-L1 expression in lobular carcinomas compared with ductal carcinomas, regardless of other pathological variables and also within the ER+HER2– group. This finding is consistent with previous descriptions in human breast cancers^{16,44} and leads us to conclude that lobular carcinomas might have a distinct pattern of TIL composition and PD-L1 activation compared with ductal carcinomas.^{45,46} Perhaps, patients diagnosed with lobular carcinoma should be allocated in specific immunotherapy trials designed apart from the ductal, given the unique morphology of their breast tumor microenvironment.

We did not identify PD-L1 expression as a factor associated with survival in patients with ER+HER2– tumors. Nevertheless, in order to verify if PD-L1 expression would have a prognostic value, we analyzed the gene expression levels of PD-L1 and PD-1 according to the MammaPrint risk classification. This prognostic tool is commonly used in the clinic to support clinical decisions especially in ER-positive breast cancer. We did not detect differences of *CD274* (PD-L1) gene expression according to the MammaPrint risk classification in luminal tumors. These results are consistent with clinical studies in which immune infiltration in ER-positive tumors has not been found to have a strong prognostic value.^{1,2} Lee et al showed that within HER2+ tumors, TILs might predict adjuvant-trastuzumab benefit only in the hormone receptor-negative/HER2+ subgroup.⁴⁷ However, the group of HER2+ tumors in our study was of limited sample size and none of the patients received trastuzumab during the period of diagnosis of our study. Within TN tumors, high PD-L1+ TIL status was significantly associated with improved BCSS and DMFS (figure 5 and supplementary figure 5 and 6). In this case, the prognostic value of PD-L1 expression reflects the strong positive correlation between PD-L1 positivity and TIL density (figure 2B and supplementary figure 2), which has been reported in many studies.^{8,9,16,17,19,21,22,26,48} TIL score is already considered to be a validated marker for prognosis in TN breast cancer.³² Further studies should test if the combination of TIL evaluation and PD-L1 expression would provide additional prognostic or predictive value.

In general, some cohort studies on breast cancer indicated that PD-L1 expression is associated with reduced survival.¹⁸⁻²¹ Other studies detected a link with better outcome in ER-negative or TN tumors,^{22-26,29} but this was not always statistically significant; while others reported no clear association.^{27,28} Controversial conclusions and large variability of the proportion of PD-L1 positivity in breast cancer may be related to the diversity of assessment methods and patient selection. Most of these studies relied on RNA levels or immunohistochemistry (IHC) using TMAs to assess PD-L1 expression. In the present study, we demonstrated the unreliability of a TMA approach (with a limited number of small cores) for PD-L1 studies in breast cancer. Consequently, our data collected by whole slide observation showed a higher percentage of PD-L1 positive breast tumors compared with studies that applied the TMA approach.^{18,19,22,23,27} Similarly, if PD-L1 expression is assessed by core-biopsies, false negative results might occur as a consequence of the heterogeneous distribution of PD-L1

expression in the tumor area.⁴⁹ It is important to mention that the archived TMAs used in this study were constructed for a different purpose than TIL evaluation. Even so, it is clear that TMAs need proper design and validation of the minimum representative area required to precisely assess tumor microenvironment features.⁵⁰

Intriguingly, the link between high PD-L1 expression and improved survival may appear contradictory since high PD-L1 expression and TIL density are also associated with ER-negativity and tumor grade 3, which are pathological features linked with poor prognosis.^{1,8,16,17,21,25,26} Here we describe an independent association between tumor grade and PD-L1 expression within TN tumors. These two associations might suggest that PD-L1 protein expression may reflect the extent of anticancer immune response in one tumor.⁴⁻⁶

Ultimately, there is an urgent need for the development of an international guide for the immune-phenotypes definition. Results of our study and emerging data^{1,3,51} point to distinct breast cancer groups or phenotypes classified according to the immune infiltration profile: tumors lacking stromal immune cells (immune-desert phenotype); tumors surrounded by focal aggregates or stromal nests of immune cells around the margins (focal/immune-excluded phenotype), and tumors containing diffuse and intratumoral infiltration of immune cells (hot/inflamed phenotype). This characterization might eventually help guide precision medicine strategies to enhance clinical response and reduce over-treatment (supplementary figure 10).

Conclusion

PD-L1 can be present in CD68+ macrophages, CD4+, FOXP3 + and CD8 + T cells of the breast tumor microenvironment. High levels of PD-L1+ TILs in TN tumors are associated with favorable prognosis. We did not find evidence that non-synonymous mutations or *BRCA1*-like status are associated with immune infiltration or PD-L1 expression in TN tumors. Immunotherapy studies in breast cancer should deal with the fact that TMAs might not provide sufficient representation of the PD-L1 status of tumors. Our data indicates that PD-L1 expression is related to the breast tumor immune infiltration. Future studies should focus on the appropriate selection of patients for anti-PD-1/PD-L1 therapy rather than focus on specific subtypes of breast cancer (e.g.TN).

Materials and methods

All work was conducted with the formal approval of the appropriate Institutional Review Boards, i.e. the Institutional Review Board of the Netherlands Cancer Institute-Antoni van Leeuwenhoek Hospital^{39,52,53} and the research ethics boards of Mount Sinai Hospital and the University Health Network, Toronto, Canada.⁵⁴ All participants of this study have given written consent, to the inclusion of material pertaining to them; acknowledged that they cannot be identified; and that data was fully anonymized. All participants of the studies had either given written consent, or secondary use of their data and

biospecimens was covered by Dutch opt-out regulations, including the National Federa-COREON Codes of Conduct: <https://www.federa.org/gedragscodes>. All patients included in the Agendia database also completed the informed consent process and were governed by central and/or local Institutional Review Boards of studies registered in Europe and USA.

Study populations and samples

Two cohorts of patients diagnosed at the Netherlands Cancer Institute-Antoni van Leeuwenhoek hospital (AVL), Amsterdam, The Netherlands, were used in this study (supplementary materials and methods). First, we included AVL patients from the ONCOPOOL cohort (n = 1,318), a retrospectively compiled database of primary operable invasive breast cancers diagnosed between 1990 and 1999.^{52,53} Inclusion criteria: women with primary operable invasive breast cancers, age at diagnosis 70 years or less. Secondly, we added AVL patients from a cohort of TN breast cancers (n = 76) that has been described previously as part of the RATHER Project (*Rational Therapy for Breast Cancer*, www.ratherproject.com).³⁹ Patients were entered when sufficient frozen tissue for DNA, RNA and protein isolation were available in the tissue bank. For this current study we included patients diagnosed between 1985 and 2007.

Both cohorts are composed of patients who received primary loco-regional treatment with or without systemic adjuvant therapy. We aimed to perform PD-L1 staining on tumors of TN RATHER patients, all ER-negative patients from ONCOPOOL and a representative selection of a third of ER-positive ONCOPOOL patients. In the analyses, patients were classified by the common breast cancer subtypes: ER+HER2- (n = 162), HER2+ (n = 101) and TN (n = 147; supplementary materials and methods). Description of data collection, TMA constructions and other details of the cohorts are provided in the supplementary materials and methods.

A selection of primary breast tumor material from female patients from the Ontario Familial Breast Cancer Registry (OFBCR),⁵⁵ the Ontario site of the Breast Cancer Family Registry (BCFR),⁵⁴ diagnosed between 1996–2005, was used as an independent cohort to validate the association between the scores and pathological variables. In total, 144 tumors from different subtypes were stained for PD-L1 and analyzed according to histopathological variables (supplementary materials and methods).

We assessed gene expression data from 547 breast tumors from patients included in several clinical studies across Europe and USA, in which MammaPrint gene profile data was collected and stored at Agendia. All breast cancer samples were processed at Agendia central laboratories and were treatment-naïve when the MammaPrint assay was performed. Molecular breast cancer subtypes were classified as luminal, HER2-like and basal using the BluePrint gene profile. MammaPrint and BluePrint were performed using RNA isolated from formalin-fixed, paraffin-embedded material and their indices of classification were calculated as previously described.^{36,37,56} Description of the gene expression assays is available in the supplementary materials and methods.

PD-L1 immunohistochemistry and TIL evaluation

IHC assays were performed using rabbit anti-human PD-L1 antibody, clone E1L3N XP[®] (Cell Signaling). Detailed experimental procedures are described in supplementary materials and methods.

Certified pathologists (KVdV, JS and ACM) performed the evaluation of TILs on full whole slide sections of the PD-L1 IHC or hematoxylin & eosin stain. Scoring was based on the recommended methodology of the International TILs Working Group.³² Briefly, the percentage of stromal TILs was determined by the area occupied by mononuclear inflammatory cells over total intratumoral stromal area within the borders of the invasive tumor (including the invasive tumor front). Tutorials and training-modules to train pathologists to score TILs are available on-line: <https://www.tilsinbreastcancer.org>. The density of stromal TILs was recorded as a continuous percentage and categorized for analyses as: none or focal TILs if < 5%, low in between 5–50%, and high if > 50%.

A dedicated breast and immuno-pathologist (KvdV) scored PD-L1 expression in whole slides and TMAs. The percentage of PD-L1-positive tumor cells (PD-L1+ tumor-cells) exhibiting membrane staining over the entire tumor was recorded as a continuous variable (0 – 100%) and categorized for analyses as: negative if < 1% and positive if ≥ 1%. The percentage of PD-L1-positive tumor-infiltrating lymphocytes (PD-L1 + TILs) was based on the percentage of the area occupied by stromal TILs exhibiting PD-L1 staining over the total area occupied by stromal TILs (0 – 90%; as continuous variable). It was categorized as: negative or focal if < 5%, moderate in between 5–50%, and high if > 50%. Further details of the validation of the scoring methodology are provided in the supplementary materials and methods.

Multiplex automated image acquisition and analysis

Multispectral images were generated using the Perkin Elmer Vectra 3.0 microscope (PerkinElmer, Hopkinton, MA) based on immunofluorescence (IF) staining of multiple markers: CD4, CD68, CD8, pan-cytokeratin (CK), FOXP3, DAPI and PD-L1 (antibodies and staining methods detailed in the supplementary materials and methods). Multispectral image cubes (8-bit) were acquired with 20x objective lens (0.5 micron/pixel). Each image consisted of an area around $1.7 \times 10^6 \mu\text{m}^2$. A self-learning algorithm built by inForm Advanced Image Analysis software (Perkin Elmer) was used to quantify the cells of each image, quantify the intensity of the markers per cell, and phenotype each of the cells as CD4+ (T helper; FOXP3-), CD68+ (macrophages), CD8+ (T cytotoxic), FOXP3+ (T regulatory; co-expressing CD4), or tumor (CK+) cells. Stromal cells without any immune marker or CK expression were classified as other cells (only DAPI+). The percentage of PD-L1-positive cells was measured using a threshold on the PD-L1 spectral intensity captured by the image analysis [negative if quantitative immunofluorescence (QIF) < 7 or positive if QIF ≥ 7]. Certified pathologists (KVdV and HH) and immune-pathologist (EH)

supervised all the steps of the image analysis process. Further details of the validation of the phenotype classification are provided in the supplementary materials and methods.

BRCA1-like classification

We retrieved previously published data on *BRCA1*-like classification³⁹ and tumor mutation analysis⁵¹ from the TN tumors from RATHER cohort (n = 56). DNA had been isolated from frozen tumors (30 x 30 μ m sections) using the DNeasy kit for purification of total DNA (Qiagen). Tumor DNA had been used to access *BRCA1*-like classification using MLPA (multiplex ligation-dependent probe amplification), detailed in previous publications^{38,39} and in the supplementary materials and methods.

Tumor mutation analysis

Instructions about sequencing of the RATHER cohort samples have been detailed in Michaut et al.⁵¹ In short, DNA sequencing was performed on an Illumina HiSeq 2000 platform. For each sample, Illumina TruSeq index libraries were constructed according to manufacturer's instructions before being enriched by capture with a biotinylated RNA probe set targeting 613 genes: 518 protein kinases and 95 additional cancer genes, including *BRCA1* and *BRCA2* (Agilent Technologies, 3.2 Mb), listed in the supplementary materials and methods. We split the set of all candidate somatic variants into 2 categories: non-silent somatic mutations (protein-altering) and silent somatic mutations (not-protein-altering).

Statistical analyses

Comparisons of means between two groups were examined by Student's *t*-test and between 3 or more groups by ANOVA. Degree of association between pathological scores and mutation levels were analyzed by Spearman's rank correlation test. The intraclass correlation coefficient (ICC) was used to quantify the degree to which immune scores from different observers agree with each other, assuming two-way random single measures⁵⁷. Associations between PD-L1 positivity and histopathological variables were evaluated by the *Chi*-square test. Odds ratios (OR) with their respective 95% confidence intervals (95% CI) were calculated using binomial logistic regression models adjusted for the following independent clinical variables: age at diagnosis (per year); tumor grade (grade 1 and 2 versus grade 3); tumor size (per cm); lymph node metastasis (per number of involved lymph nodes); and, if applicable, ER and PR status (negative versus positive) or the study of origin (ONCOPOOL versus RATHER). Morphology (ductal, lobular or other types) was added as an independent clinical variable only in ER+HER2-, due the large proportion of ductal type in the ER-negative group (HER2+ and TN).

Breast cancer specific survival (BCSS) time was calculated from the date of diagnosis. End of follow up was defined as the date of death caused by breast cancer progression or treatment related, last or 10-years follow up (censoring),

whatever came first. Hazard ratios (HRs) were estimated using Cox regression models and stratified by studies when applicable. For distant metastasis-free survival (DMFS) time was calculated from the date of diagnosis. End of follow up was defined as the date of the diagnosis of metastatic breast tumor cells in another organ, last follow up or death or 10 years time (censoring), whatever came first.

Multivariable Cox models were fitted including age at diagnosis (per year); tumor grade (grade 1 plus 2 versus grade 3); tumor size (per cm); lymph node metastasis (per number of involved lymph nodes), and the adjuvant treatment variables: chemotherapy, endocrine therapy and radiotherapy (classified by the categories: not treated versus treated). Morphology type (ductal, lobular or other types), ER and PR status (negative versus positive) were included as co-variables in the analyses of ER+HER2- and HER2+ groups. All results were obtained from complete case analysis. All P-values reported are from two-sided tests and the threshold for significance was set at $p = 0.05$. All statistical analyses were performed using RStudio version 3.2.3 (RStudio Team, 2015).

Acknowledgments

The authors thank all the many patients and families who contributed to this study; and all the researchers, clinicians, technicians and administrative staff who have enabled this work to be carried out. Special thanks goes to Philip Schouten, Sabine Linn and all members from the RATHER cohort and Sjoerd Elias for the work on the ONCOPOOL cohort. The authors would also like to acknowledge the Core Facility Molecular Pathology & Biobanking (CFMPB) and the Tumor Registry from the Netherlands Cancer Institute-Antoni van Leeuwenhoek Ziekenhuis (NKI-AVL) for the support and all those who contributed useful discussions: Bart van de Wiel, Jelle Wesseling, Mark Opdam, Jan Schellens and Rosane Vianna-Jorge.

Authors' contributions


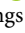

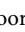






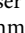
MKS, MSL and KEdV conceived the study; DP and AB selected tumor blocks and stained; GKJH and MJvdV carried PD-L1 staining. KVdV, HH, ACM and JS scored the tumors; RvdL, EH, DP, AB, KVdV, HH and MSL generated, interpreted, supervised or analyzed the multiplex images. AMG, DW, RB and LM generated and interpreted gene expression data. KK, TMS, MM and RB generated and interpreted data from RATHER cohort. AMM, NW and ILA provided material and data from OFBCR cohort. MSL performed the analyses, interpreted the data and wrote the paper under supervision of MKS, KEdV and MK. All other authors contributed data and/or materials; all authors critically commented and approved the final version of the manuscript.

Funding

ONCOPOOL was supported by a European Commission Framework 5 Project Grant. RATHER was supported by European Commission Framework 7 Project Grant. MSL received a scholarship from Science without Borders - CAPES. Funding of group Schmidt at the Netherlands Cancer Institute provided a partial grant and covered the IHC staining and image analysis. This work was also supported by grant UM1 CA164920 from the USA National Cancer Institute. The content of this manuscript does not necessarily reflect the views or policies of the National Cancer Institute or any of the collaborating centers in the Breast Cancer Family Registry (BCFR), nor does mention of trade names, commercial products, or organizations imply endorsement by the USA Government or the BCFR. I.L. Andrulis holds the Anne and

Max Tanenbaum Chair in Molecular Medicine at Mount Sinai Hospital of the Sinai Health System and the University of Toronto.

ORCID

Marcelo Sobral-Leite  <http://orcid.org/0000-0002-4275-8050>
 Koen Van de Vijver  <http://orcid.org/0000-0002-2026-9790>
 Magali Michaut  <http://orcid.org/0000-0003-2002-2277>
 Hugo M. Horlings  <http://orcid.org/0000-0003-4782-8828>
 Tesa M. Severson  <http://orcid.org/0000-0002-7568-4705>
 Nayana Weerasooriya  <http://orcid.org/0000-0003-2907-4380>
 Joyce Sanders  <http://orcid.org/0000-0002-0551-7813>
 Annuska M Glas  <http://orcid.org/0000-0002-0775-138X>
 Erik Hooijberg  <http://orcid.org/0000-0002-4482-2191>
 Rene Bernards  <http://orcid.org/0000-0001-8677-3423>
 Marleen Kok  <http://orcid.org/0000-0001-9043-9815>
 Karin E. de Visser  <http://orcid.org/0000-0002-0293-868X>
 Marjanka K. Schmidt  <http://orcid.org/0000-0002-2228-429X>

References

- Savas P, Salgado R, Denkert C, Sotiriou C, Darcy PK, Smyth MJ, Loi S. Clinical relevance of host immunity in breast cancer: from TILs to the clinic. *Nat Rev Clin Oncol*. 2016;13:228–241. PMID:26667975. doi: 10.1038/nrclinonc.2015.215.
- Dieci MV, Griguolo G, Miglietta F, Guarneri V. The immune system and hormone-receptor positive breast cancer: is it really a dead end? *Cancer Treatment Reviews*. 2016;46:9–19. PMID:27055087. doi: 10.1016/j.ctrv.2016.03.011.
- Chen DS, Mellman I. Elements of cancer immunity and the cancer-immune set point. *Nature*. 2017;541:321–330. PMID:28102259. doi: 10.1038/nature21349.
- Freeman GJ, Long AJ, Iwai N, Bourque K, Chernova T, Nishimura H, Fitz LJ, Malenkovich N, Okazaki T, Byrne MC, et al. Engagement of the PD-1 immunoinhibitory receptor by a novel B7 family member leads to negative regulation of lymphocyte activation. *The Journal of Experimental Medicine*. 2000;192:10.1084/jem.192.7.102727–34. PMID:11015443.
- Okazaki T, The HT. PD-1-PD-L pathway in immunological tolerance. *Trends in Immunology*. 2006;27:195–201. PMID:16500147. doi: 10.1016/j.it.2006.02.001.
- Taube JM, Anders RA, Young GD, Xu H, Sharma R, McMiller TL, Chen S, Klein AP, Pardoll DM, Topalian SL, et al. Colocalization of inflammatory response with B7-H1 expression in human melanocytic lesions supports an adaptive resistance mechanism of immune escape. *Science Translational Medicine*. 2012;4:127ra37–ra37. PMID:22461641. doi: 10.1126/scitranslmed.3003689.
- Mezzadra R, Sun C, Jae LT, Gomez-Eerland R, De Vries E, Wu W, Logtenberg MEW, Slagter M, Rozeman EA, Hofland I, et al. Identification of CMTM6 and CMTM4 as PD-L1 protein regulators. *Nature*. 2017;549:106–110. PMID:28813410. doi: 10.1038/nature23669.
- Wang X, Teng F, Kong L, Yu J. PD-L1 expression in human cancers and its association with clinical outcomes. *OncoTargets and Therapy*. 2016;9:5023–5039. PMID:27574444. doi: 10.2147/ott.s105862.
- Wu P, Wu D, Li L, Chai Y, Huang J. PD-L1 and survival in solid tumors: A meta-analysis. *PLoS one*. 2015;10:e0131403. PMID:26114883. doi: 10.1371/journal.pone.0131403.
- Robert C, Thomas L, Bondarenko I, O'Day S, Weber J, Garbe C, Lebbe C, Baurain J-F, Testori A, Grob -J-J, et al. Ipilimumab plus dacarbazine for previously untreated metastatic melanoma. *The New England Journal of Medicine*. 2011;364:2517–2526. PMID:21639810. doi: 10.1056/NEJMoa1104621.
- Bustamante Alvarez JG, Gonzalez-Cao M, Karachaliou N, Santarpia M, Viteri S, Teixeira C, Rosell R. Advances in immunotherapy for treatment of lung cancer. *Cancer Biology & Medicine*. 2015;12:209–222. PMID:26487966. doi: 10.7497/j.issn.2095-3941.2015.0032.
- Brahmer JR, Tykodi SS, Chow LQ, Hwu WJ, Topalian SL, Hwu P, Drake CG, Camacho LH, Kauh J, Odunsi K, et al. Safety and activity of anti-PD-L1 antibody in patients with advanced cancer. *The New England Journal of Medicine*. 2012;366:2455–2465. PMID:22658128. doi: 10.1056/NEJMoa1200694.
- Pardoll DM. The blockade of immune checkpoints in cancer immunotherapy. *Nature Reviews Cancer*. 2012;12:252–264. PMID:22437870. doi: 10.1038/nrc3239.
- Emens LA, Kok M, Ojalvo LS. Targeting the programmed cell death-1 pathway in breast and ovarian cancer. *Current Opinion in Obstetrics & Gynecology*. 2016;28:142–147. PMID:26881392. doi: 10.1097/gco.0000000000000257.
- Saha P, Nanda R. Concepts and targets in triple-negative breast cancer: recent results and clinical implications. *Therapeutic Advances in Medical Oncology*. 2016;8:351–359. PMID:27583027. doi: 10.1177/1758834016657071.
- Buisseret L, Garaud S, De Wind A, Van Den Eynden G, Boisson A, Solinas C, Gu-Trantien C, Naveaux C, Lodewyckx J-N, Duvillier H, et al. Tumor-infiltrating lymphocyte composition, organization and PD-1/PD-L1 expression are linked in breast cancer. *Oncoimmunology*. 2017;6:e1257452. PMID:28197375. doi: 10.1080/2162402x.2016.1257452.
- Cimino-Mathews A, Thompson E, Taube JM, Ye X, Lu Y, Meeker A, Xu H, Sharma R, Lecksel K, Cornish TC, et al. PD-L1 (B7-H1) expression and the immune tumor microenvironment in primary and metastatic breast carcinomas. *Human Pathology*. 2015;47:52–63. PMID:26527522. doi: 10.1016/j.humpath.2015.09.003.
- Muenst S, Schærli AR, Gao F, Daster S, Trella E, Droeser RA, Muraro MG, Zajac P, Zanetti R, Gillanders WE, et al. Expression of programmed death ligand 1 (PD-L1) is associated with poor prognosis in human breast cancer. *Breast Cancer Research and Treatment*. 2014;146:15–24. PMID:24842267. doi: 10.1007/s10549-014-2988-5.
- Polonia A, Pinto R, Cameselle-Teijeiro JF, Schmitt FC, Paredes J. Prognostic value of stromal tumour infiltrating lymphocytes and programmed cell death-ligand 1 expression in breast cancer. *Journal of Clinical Pathology*. 2017;70:860–867. PMID:28373294. doi: 10.1136/jclinpath-2016-203990.
- Qin T, Zeng YD, Qin G, Xu F, Lu JB, Fang WF, Xue C, Zhan J-H, Zhang X-K, Zheng Q-F, et al. High PD-L1 expression was associated with poor prognosis in 870 Chinese patients with breast cancer. *Oncotarget*. 2015;6:33972–33981. PMID:26378017. doi: 10.18632/oncotarget.5583.
- Tsang JY, Au WL, Lo KY, Ni YB, Hlaing T, Hu J, Chan S-K, Chan K-F, Cheung S-Y, Tse GM. PD-L1 expression and tumor infiltrating PD-1+ lymphocytes associated with outcome in HER2+ breast cancer patients. *Breast Cancer Research and Treatment*. 2017;162:19–30. PMID:28058578. doi: 10.1007/s10549-016-4095-2.
- Ali HR, Glont SE, Blows FM, Provenzano E, Dawson SJ, Liu B, Hiller L, Dunn J, Poole CJ, Bowden S, et al. PD-L1 protein expression in breast cancer is rare, enriched in basal-like tumours and associated with infiltrating lymphocytes. *Annals of Oncology: Official Journal of the European Society for Medical Oncology/ESMO*. 2015;26:1488–1493. PMID:25897014. doi: 10.1093/annonc/mdv192.
- Baptista MZ, Sarian LO, Derchain SF, Pinto GA, Vassallo J. Prognostic significance of PD-L1 and PD-L2 in breast cancer. *Human Pathology*. 2015;47:78–84. PMID:26541326. doi: 10.1016/j.humpath.2015.09.006.
- Botti G, Collina F, Scognamiglio G, Rao F, Peluso V, De Cecio R, Piezzo M, Landi G, De Laurentiis M, Cantile M, et al. Programmed death ligand 1 (PD-L1) tumor expression is associated with a better prognosis and diabetic disease in triple

- negative breast cancer patients. *International Journal of Molecular Sciences*. 2017;18. PMID:28230773. doi: [10.3390/ijms18020459](https://doi.org/10.3390/ijms18020459).
25. Guo L, Li W, Zhu X, Ling Y, Qiu T, Dong L, Fang Y, Yang H, Ying J. PD-L1 expression and CD274 gene alteration in triple-negative breast cancer: implication for prognostic biomarker. *SpringerPlus*. 2016;5:805. PMID:27390646. doi: [10.1186/s40064-016-2513-x](https://doi.org/10.1186/s40064-016-2513-x).
 26. Schalper KA, Velcheti V, Carvajal D, Wimberly H, Brown J, Puztai L, Rimm DL. In situ tumor PD-L1 mRNA expression is associated with increased TILs and better outcome in breast carcinomas. *Clinical Cancer Research: an Official Journal of the American Association for Cancer Research*. 2014;20:2773–2782. PMID:24647569. doi: [10.1158/1078-0432.ccr-13-2702](https://doi.org/10.1158/1078-0432.ccr-13-2702).
 27. Beckers RK, Selinger CI, Vilain R, Madore J, Wilmott JS, Harvey K, Holliday A, Cooper CL, Robbins E, Gillett D, et al. Programmed death ligand 1 expression in triple-negative breast cancer is associated with tumour-infiltrating lymphocytes and improved outcome. *Histopathology*. 2016;69:25–34. PMID:26588661. doi: [10.1111/his.12904](https://doi.org/10.1111/his.12904).
 28. Park IH, Kong SY, Ro JY, Kwon Y, Kang JH, Mo HJ, Jung S-Y, Lee S, Lee KS, Kang H-S, et al. Prognostic implications of tumor-infiltrating lymphocytes in association with programmed death ligand 1 expression in early-stage breast cancer. *Clinical Breast Cancer*. 2016;16:51–58. PMID:26364145. doi: [10.1016/j.clbc.2015.07.006](https://doi.org/10.1016/j.clbc.2015.07.006).
 29. Sabatier R, Finetti P, Mamessier E, Adelaide J, Chaffanet M, Ali HR, Viens P, Caldas C, Birnbaum D, Bertucci F. Prognostic and predictive value of PDL1 expression in breast cancer. *Oncotarget*. 2015;6:5449–5464. PMID:25669979. doi: [10.18632/oncotarget.3216](https://doi.org/10.18632/oncotarget.3216).
 30. Budczies J, Bockmayr M, Denkert C, Klauschen F, Lennerz JK, Györfy B, Dietel M, Loibl S, Weichert W, Stenzinger A. Classical pathology and mutational load of breast cancer - integration of two worlds. *The Journal of Pathology Clinical Research*. 2015;1:225–238. PMID:27499907. doi: [10.1002/cjp.2.25](https://doi.org/10.1002/cjp.2.25).
 31. Luen S, Virassamy B, Savas P, Salgado R, Loi S. The genomic landscape of breast cancer and its interaction with host immunity. *Breast*. 2016;29:241–250. PMID:27481651. doi: [10.1016/j.breast.2016.07.015](https://doi.org/10.1016/j.breast.2016.07.015).
 32. Salgado R, Denkert C, Demaria S, Sirtaine N, Klauschen F, Pruneri G, Wienert S, Van Den Eynden G, Baehner FL, Penault-Llorca F, et al. The evaluation of tumor-infiltrating lymphocytes (TILs) in breast cancer: recommendations by an International TILs Working Group 2014. *Annals of Oncology: Official Journal of the European Society for Medical Oncology/ESMO*. 2015;26:259–271. PMID:25214542. doi: [10.1093/annonc/mdu450](https://doi.org/10.1093/annonc/mdu450).
 33. Dunn GP, Bruce AT, Ikeda H, Old LJ, Schreiber RD. Cancer immunoevasion: from immunosurveillance to tumor escape. *Nature Immunology*. 2002;3:991–998. PMID:12407406. doi: [10.1038/ni1102-991](https://doi.org/10.1038/ni1102-991).
 34. Ali HR, Provenzano E, Dawson SJ, Blows FM, Liu B, Shah M, Earl HM, Poole CJ, Hiller L, Dunn JA, et al. Association between CD8+ T-cell infiltration and breast cancer survival in 12,439 patients. *Annals of Oncology: Official Journal of the European Society for Medical Oncology/ESMO*. 2014;25(8):1536–1543. PMID:24915873. doi: [10.1093/annonc/mdu191](https://doi.org/10.1093/annonc/mdu191).
 35. Cardoso F, Van't Veer LJ, Bogaerts J, Slaets L, Viale G, Delaloge S, Pierga J-Y, Brain E, Causeret S, DeLorenzi M, et al. 70-gene signature as an aid to treatment decisions in early-stage breast cancer. *The New England Journal of Medicine*. 2016;375:717–729. PMID:27557300. doi: [10.1056/NEJMoa1602253](https://doi.org/10.1056/NEJMoa1602253).
 36. Beumer I, Witteveen A, Delahaye L, Wehkamp D, Snel M, Dreezen C, Zheng J, Floore A, Brink G, Chan B, et al. Equivalence of MammaPrint array types in clinical trials and diagnostics. *Breast Cancer Research and Treatment*. 2016;156:279–287. PMID:27002507. doi: [10.1007/s10549-016-3764-5](https://doi.org/10.1007/s10549-016-3764-5).
 37. Krijgsman O, Roepman P, Zwart W, Carroll JS, Tian S, De Snoo FA, Bender RA, Bernards R, Glas AM. A diagnostic gene profile for molecular subtyping of breast cancer associated with treatment response. *Breast Cancer Research and Treatment*. 2012;133:37–47. PMID:21814749. doi: [10.1007/s10549-011-1683-z](https://doi.org/10.1007/s10549-011-1683-z).
 38. Lips EH, Laddach N, Savola SP, Vollebbergh MA, Oonk AM, Imholz AL, Wessels LF, Wesseling J, Nederlof PM, Rodenhuis S. Quantitative copy number analysis by multiplex ligation-dependent probe amplification (MLPA) of BRCA1-associated breast cancer regions identifies BRCAness. *Breast Cancer Research: BCR*. 2011;13:R107. PMID:22032731. doi: [10.1186/bcr3049](https://doi.org/10.1186/bcr3049).
 39. Severson TM, Peeters J, Majewski I, Michaut M, Bosma A, Schouten PC, Chin S-F, Pereira B, Goldgraben MA, Bismeyer T, et al. BRCA1-like signature in triple negative breast cancer: molecular and clinical characterization reveals subgroups with therapeutic potential. *Molecular Oncology*. 2015;9:1528–1538. PMID:26004083. doi: [10.1016/j.molonc.2015.04.011](https://doi.org/10.1016/j.molonc.2015.04.011).
 40. Nolan E, Savas P, Policheni AN, Darcy PK, Vaillant F, Mintoff CP, Dushyanthen S, Mansour M, Pang J-MB, Fox SB, et al. Combined immune checkpoint blockade as a therapeutic strategy for BRCA1-mutated breast cancer. *Science Translational Medicine*. 2017;9:eaal4922. PMID:28592566. doi: [10.1126/scitranslmed.aal4922](https://doi.org/10.1126/scitranslmed.aal4922).
 41. Smid M, Rodriguez-Gonzalez FG, Sieuwerts AM, Salgado R, Prager-Van Der Smissen WJ, Vlugt-Daane MV, Nik-Zainal S, Staaf J, Brinkman AB. Breast cancer genome and transcriptome integration implicates specific mutational signatures with immune cell infiltration. *Nature Communications*. 2016;7:12910. PMID:27666519. doi: [10.1038/ncomms12910](https://doi.org/10.1038/ncomms12910).
 42. Turajlic S, Litchfield K, Xu H, Rosenthal R, McGranahan N, Ji R, Wong YNS, Rowan A, Kanu N, Al Bakir M, et al. Insertion-and-deletion-derived tumour-specific neoantigens and the immunogenic phenotype: a pan-cancer analysis. *The Lancet Oncology*. 2017;18:1009–1021. PMID:28694034. doi: [10.1016/s1470-2045\(17\)30516-8](https://doi.org/10.1016/s1470-2045(17)30516-8).
 43. Solinas C, Marcoux D, Garaud S, Van Den Eynden G, De Wind A, Boisson A, Larsimont D, Piccart M, Roodenbeke DK, Willard-Gallo K. BRCA gene mutations do not shape the extent and organization of tumor infiltrating lymphocytes in high-risk triple negative breast cancer. *San Antonio Breast Cancer Symposium 2016; P2*;
 44. Drosier R, Zlobec I, Kilic E, Guth U, Heberer M, Spagnoli G, Oertli D, Tapia C. Differential pattern and prognostic significance of CD4+, FOXP3+ and IL-17+ tumor infiltrating lymphocytes in ductal and lobular breast cancers. *BMC Cancer*. 2012;12:134. PMID:22471961. doi: [10.1186/1471-2407-12-134](https://doi.org/10.1186/1471-2407-12-134).
 45. Desmedt C, Salgado R, Fornili M, Pruneri G, Van Den Eynden G, Zoppoli G, Rothé F, Buisseret L, Garaud S, Willard-Gallo K, et al. Immune infiltration in invasive lobular breast cancer. *Journal of the National Cancer Institute*. 2018;110:768–776. PMID:29471435. doi: [10.1093/jnci/djx268](https://doi.org/10.1093/jnci/djx268).
 46. Thompson ED, Taube JM, Asch-Kendrick RJ, Ogurtsova A, Xu H, Sharma R, Meeker A, Argani P, Emens LA, Cimino-Mathews A. PD-L1 expression and the immune microenvironment in primary invasive lobular carcinomas of the breast. *Modern Pathology: an Official Journal of the United States and Canadian Academy of Pathology, Inc*. 2017;30:1551–1560. PMID:28731046. doi: [10.1038/modpathol.2017.79](https://doi.org/10.1038/modpathol.2017.79).
 47. Lee HJ, Kim JY, Park IA, Song IH, Yu JH, Ahn JH, Gong G. Prognostic significance of tumor-infiltrating lymphocytes and the tertiary lymphoid structures in HER2-positive breast cancer treated with adjuvant trastuzumab. *American Journal of Clinical Pathology*. 2015;144:278–288. PMID:26185313. doi: [10.1309/ajcpixuydvz0rz3g](https://doi.org/10.1309/ajcpixuydvz0rz3g).
 48. Taube JM, Klein A, Brahmer JR, Xu H, Pan X, Kim JH, Chen L, Pardoll DM, Topalian SL, Anders RA. Association of PD-1, PD-1 ligands, and other features of the tumor immune microenvironment with response to anti-PD-1 therapy. *Clinical Cancer Research: an Official Journal of the American Association for Cancer Research*. 2014;20:5064–5074. PMID:24714771. doi: [10.1158/1078-0432.ccr-13-3271](https://doi.org/10.1158/1078-0432.ccr-13-3271).
 49. Li C, Huang C, Mok TS, Zhuang W, Xu H, Miao Q, Fan X, Zhu W, Huang Y, Lin X, et al. Comparison of 22C3 PD-L1 expression between surgically resected specimens and paired tissue microarrays in non-small cell lung cancer. *Journal of Thoracic Oncology*:

- Official Publication of the International Association for the Study of Lung Cancer. 2017;12:1536–1543. PMID:28751245. doi: [10.1016/j.jtho.2017.07.015](https://doi.org/10.1016/j.jtho.2017.07.015).
50. Rehman JA, Han G, Carvajal-Hausdorf DE, Wasserman BE, Pelekanou V, Mani NL, McLaughlin J, Schalper KA, Rimm DL. Quantitative and pathologist-read comparison of the heterogeneity of programmed death-ligand 1(PD-L1) expression in non-small cell lung cancer. *Modern Pathology: an Official Journal of the United States and Canadian Academy of Pathology, Inc.* 2017;30:340–349. PMID:27834350. doi: [10.1038/modpathol.2016.186](https://doi.org/10.1038/modpathol.2016.186).
 51. Michaut M, Chin SF, Majewski I, Severson TM, Bismeyer T, De Koning L, Peeters JK, Schouten PC, Rueda OM, Bosma AJ, et al. Integration of genomic, transcriptomic and proteomic data identifies two biologically distinct subtypes of invasive lobular breast cancer. *Scientific Reports.* 2016;6:18517. PMID:26729235. doi: [10.1038/srep18517](https://doi.org/10.1038/srep18517).
 52. Blamey RW, Hornmark-Stenstam B, Ball G, Blichert-Toft M, Cataliotti L, Fourquet A, Gee J, Holli K, Jakesz R, Kerin M, et al. ONCOPOOL - a European database for 16,944 cases of breast cancer. *European Journal of Cancer.* 2010;46:56–71. PMID:19811907. doi: [10.1016/j.ejca.2009.09.009](https://doi.org/10.1016/j.ejca.2009.09.009).
 53. Roewe T, Sobral-Leite M, Dekker TJA, Wesseling J, Smit V, Tollenaar R, Schmidt MK, Mesker WE. The prognostic value of the tumour-stroma ratio in primary operable invasive cancer of the breast: a validation study. *Breast Cancer Research and Treatment.* 2017;166:435–445. PMID:28795248. doi: [10.1007/s10549-017-4445-8](https://doi.org/10.1007/s10549-017-4445-8).
 54. John EM, Hopper JL, Beck JC, Knight JA, Neuhausen SL, Senie RT, Ziogas A, Andrulis IL, Anton-Culver H, Boyd N, et al. The breast cancer family registry: An infrastructure for cooperative multinational, interdisciplinary and translational studies of the genetic epidemiology of breast cancer. *Breast Cancer Research: BCR.* 2004;6:R375–8915217505. PMID:15217505. doi: [10.1186/bcr801](https://doi.org/10.1186/bcr801).
 55. Knight JA, Sutherland HJ, Glendon G, Boyd NF, Andrulis IL; Ontario Cancer Genetics N. Characteristics associated with participation at various stages at the Ontario site of the cooperative family registry for breast cancer studies. *Annals of Epidemiology.* 2002;12:27–33. PMID:11750237. doi: [10.1016/S1047-2797\(01\)00253-8](https://doi.org/10.1016/S1047-2797(01)00253-8).
 56. Sapino A, Roepman P, Linn SC, Snel MH, Delahaye LJ, Van Den Akker J, Glas AM, Simon IM, Barth N, De Snoo FA, et al. MammaPrint molecular diagnostics on formalin-fixed, paraffin-embedded tissue. *The Journal of Molecular Diagnostics: JMD.* 2014;16:190–197. PMID:24378251. doi: [10.1016/j.jmoldx.2013.10.008](https://doi.org/10.1016/j.jmoldx.2013.10.008).
 57. Bartko JJ. The intraclass correlation coefficient as a measure of reliability. *Psychological Reports.* 1966;19:3–11. PMID:5942109. doi: [10.2466/pr0.1966.19.1.3](https://doi.org/10.2466/pr0.1966.19.1.3).